ELSEVIER

Contents lists available at ScienceDirect

# Journal of Power Sources

journal homepage: www.elsevier.com/locate/jpowsour



# Horizontally structured microbial fuel cells in yarns and woven fabrics for wearable bioenergy harvesting

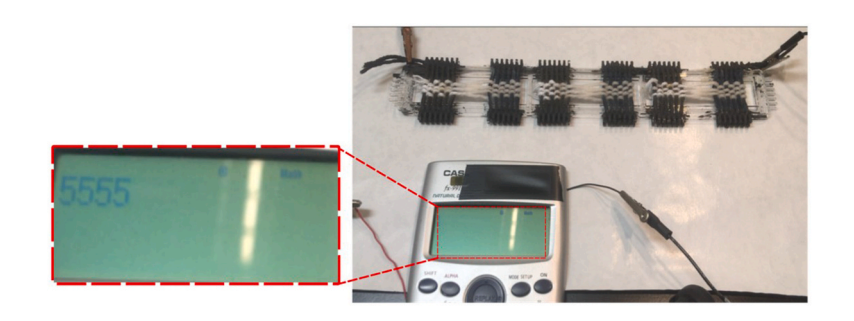
Jihyun Ryu, Yang Gao, Jong Hyun Cho, Seokheun Choi

Bioelectronics & Microsystems Laboratory, Department of Electrical & Computer Engineering, State University of New York-Binghamton, Binghamton, NY, 13902, USA

#### HIGHLIGHTS

- We create a microbial fuel cell horizontally structured in yarn and woven fabrics.
- The 1-D yarn is easily scaled up by connecting multiple yarn device units.
- The concept is extended to 2-D and 3-D textiles by weaving functional yarns.

#### GRAPHICAL ABSTRACT



## ARTICLE INFO

Keywords:
Microbial fuel cells
Wearable bioenergy harvesting
Smart textiles
Exoelectrogens
Scalable power generation

## ABSTRACT

Integration of advanced microbial fuel cell technology with conventional textile processes enables the emergence of wearable bioenergy harvesting techniques fueled by human sweat. However, without a standardized architecture for the fabrication of textile microbial fuel cells, large-scale energy harvesting from the human body with smart textiles remains elusive. In this work, a revolutionary device structure for wearable microbial fuel cells is easily built up on 1-D yarns and on 2-D and 3-D woven fabrics. The microbial fuel cell is horizontally structured on an intrinsic non-conductive yarn where the anodic and the cathodic components are formed between the pristine regions of the yarn as an ion exchange channel. The horizontally structured device in the 1-D yarn is easily scaled up to produce more power by connecting multiple yarn devices in series and parallel. The concept of the horizontally structured microbial fuel cell is extended to 2-D and 3-D wearable textiles by weaving functional yarns. The 1-D yarn device inoculated with *Shewanella oneidensis* MR-1 produced a maximum power of 452  $\mu$ A/cm³ and a current density of 47.2  $\mu$ W/cm³, which are greater than other flexible microbial fuel cells. The 2-D/3-D fabric-based devices improved the output performance enough to power an electrical calculator.

# 1. Introduction

Emerging electronics are being designed to be worn close to or attached to the human body, where they can continuously monitor health parameters and provide appropriate feedback-controlled therapeutic drug deliveries [1]. This revolution has led to the rapid development of wearable technologies, such as smart textiles, artificial electronic skins, smartwatches, electronic tattoos, and sport wristbands, by integrating small devices and functionalities into flexible and stretchable materials for seamless interfaces with the skin [2–4]. With

E-mail address: sechoi@binghamton.edu (S. Choi).

<sup>\*</sup> Corresponding author.

these intensive advancements in wearable technologies, the requirements of wearable power sources are receiving significant attention for realizing self-powered, stand-alone wearable electronics [5,6]. Energy harvesting techniques from the human body and its surroundings have been the focus of particular interest because they offer reliable, sustainable, and environmentally-friendly energy [7]. The available energy harvesting resources include mechanical energy from human motion, thermal energy from body heat, and other renewable energy such as solar irradiance and wind, which are eventually converted into useful electrical energy. Among the energy harvesting methods, producing electrochemical energy from human sweat has emerged as an ideal energy technique for powering wearable applications because sweat contains energy-rich biochemical molecules and can be easily and non-invasively sampled [7-10]. Furthermore, the recently developed iontophoretic technique enables continuous sweat extraction without exercising or controlling the environmental temperature and humidity [11]. The biochemical energy stored in sweat can be converted into electricity by using biocatalysts in a biofuel cell [8-10]. The biocatalysts in the anode of the biofuel cell oxidize biochemical molecules like lactate and glucose, which release electrons that move into the cathode through an external circuit while protons produced during oxidation transfer to the cathode through an internal ion exchange membrane. Then, the cathode collects these electrons and protons for cathodic reduction, converting the biochemical energy into electricity. The biocatalyst can be a subcellular enzyme in an enzymatic fuel cell or living microbes in a microbial fuel cell [12,13]. To date, enzymatic fuel cells have attracted more attention as a wearable biopower supply than microbial fuel cells because of concerns about microbial cytotoxicity [7]. Microbial fuel cells (MFCs) as wearable bioenergy harvesters are drawing new attention because recent research shows non-toxic human-body inhabiting bacteria can produce electricity while being long-term self-sustainable [12-14]. A flexible and stretchable microbial fuel cell was previously developed by monolithically integrating components into a single sheet of textile substrate [15,16]. This single-layer textile MFC used Pseudomonas aeruginosa PAO1 as a biocatalyst to provide a stable power performance despite repeated stretching and twisting. A two-yarn microbial fuel cell consisting of one anodic yarn and another cathodic yarn was constructed, which could be used as a battery configured as a bracelet [17]. Very recently, the science journal Nano Energy published an article about the discovery of the electrogenicity of several skin-inhabiting bacteria including Staphylococcus epidermidis, Staphylococcus capitis, and Micrococcus luteus, which demonstrated significant power generation by a skin-mountable paper-based microbial fuel cell [14]. However, wearable microbial fuel cells have been usually ignored as a power source and are at an early development stage. Above all, the device has no standardized architecture for the fabrication of a flexible, and wearable microbial fuel cell and its scalable format with series and parallel connections. Even the latest advances in wearable microbial fuel cells require an innovative strategy to revolutionize the device platform and configuration for greater power performance with increasing device dimensions [14,17].

In this work, we propose a revolutionary and standardizable device structure for wearable microbial fuel cells that can be readily built up on 1-D yarns and on 2-D and 3-D woven fabrics for larger smart textiles. The yarn- and fabric-based platforms can create a unique opportunity for liquid-containing microbial fuel cell technology because of their excellent wicking force to contain and transport aqueous reagents such as bacterial inoculum and electrolyte. Furthermore, the hydrophilic nature of the yarn and fabric along with their extremely large surface area ensures a large area for bacteria to attach, leading to significant power enhancement. The microbial fuel cell is horizontally structured on an intrinsic non-conductive yarn where the anodic and the cathodic components are formed in the pristine region of the yarn. A conformal coating of conductive polymer, poly(3,4-ethylenedioxythiophene) polystyrene sulfonate (PEDOT:PSS), on the yarn defines micro-porous conductive electrodes with a large and accessible surface area that

enables superior electrocatalytic electrode activity [15,16]. Ag<sub>2</sub>O catalyst is added to the cathode for the cathodic reduction reaction [18]. The pristine region between the anode and the cathode acts as the ion exchange membrane when it absorbs an electrolyte such as human sweat. The microbial fuel cell horizontally structured in 1-D yarn can be easily scaled up to produce more power by connecting multiple yarn devices in series and parallel. On the other hand, conductive anodic and cathodic varns can be respectively prepared by coating the entire length of the yarns with selective anodic and cathodic functional materials. These functional yarns as weft and non-conductive pristine yarns as warp can be woven together into a large conductive fabric anode and cathode while the remaining pristine fabric region between them forming a horizontally structured 2-D microbial fuel cell. The 2-D fuel cells can be connected in series based on the warp yarns or in parallel by stacking multiple 2-D devices, forming a 3-D microbial fuel cell. To verify the viability of our novel 1-D, 2-D, and 3-D platforms as power supplies, a well-known exoelectrogen, Shewanella oneidensis MR-1, is used as a biocatalyst. This horizontal structure of the microbial fuel cell provides a versatile, flexible, and configurable design for different dimensions and offer a large-scale wearable application platform.

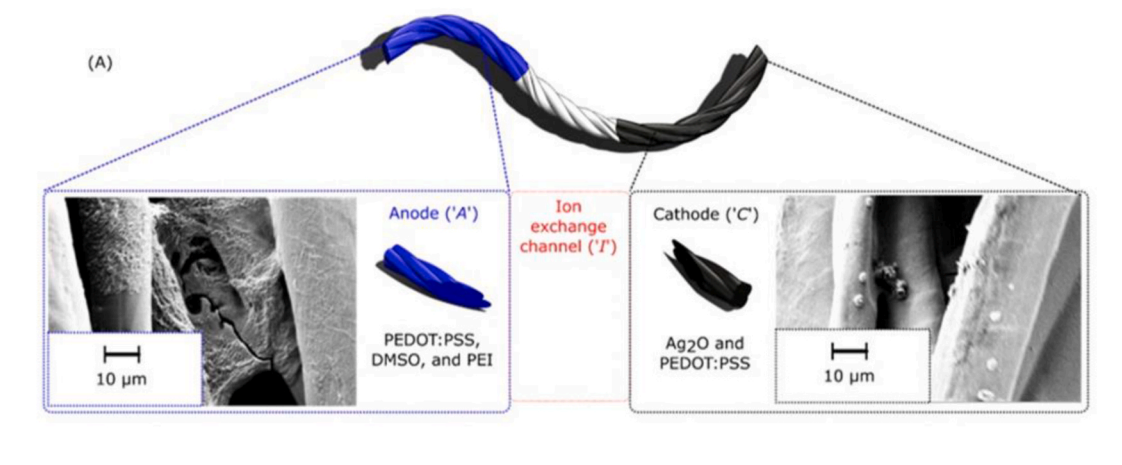
#### 2. Results and discussion

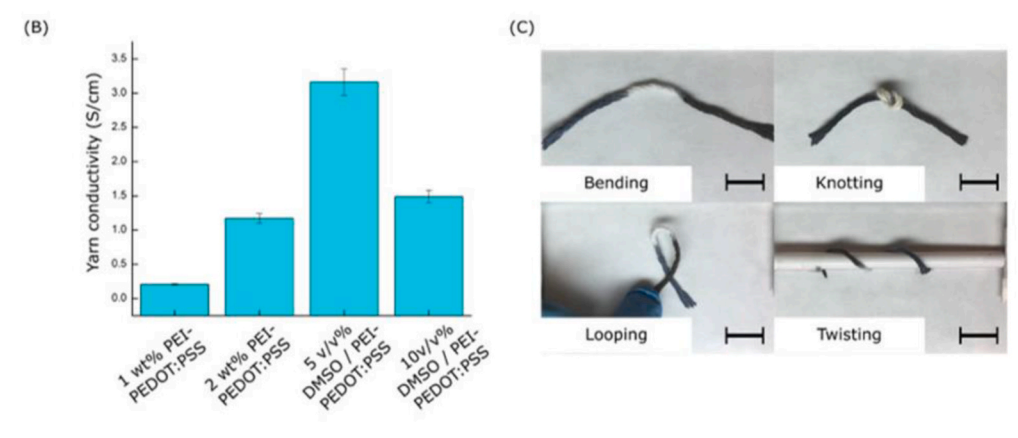
## 2.1. 1-D yarn microbial fuel cell

A commercially available yarn composed of 70% cotton and 30% polyethylene terephthalate was used as a fundamental substrate for the 1-D yarn-based microbial fuel cell. Fig. 1A shows how we used insulating and hydrophilic yarn to build the MFC. Poly(ethlylenemine)-PEDOT:PSS coated the 25-mm anode (A), and Ag<sub>2</sub>O-PEDOT:PSS coated the 25-mm long cathode (C). The 20-mm pristine region between the electrodes served as an ion-exchange channel (I). PEDOT:PSS has been widely used as a conductive biocompatible coating material to allow electrical conductivity in non-conducting fibers, yarns, and textiles for biomaterials [18-20]. The introduction of poly(ethlylenemine) into the PEDOT:PSS can improve the bacterial electron transfer efficiency by reducing the work function of PEDOT:PSS, but this decreases the conductivity [21]. The conductivity of poly(ethlylenemine)-PEDOT:PSS was improved by treatment with a polar organic solvent, dimethyl sulfoxide (DMSO) (Fig. 1B) [22]. The concentration of the poly(ethlylenemine)-PEDOT: PSS mixture from 1 wt% to 2 wt% in the yarn increased its conductivity from 0.2 S cm<sup>-1</sup> to 1.2 S cm<sup>-1</sup>, which is not sufficient for electrode applications in a MFC. Conductivity was enhanced (3.2 S cm<sup>-1</sup>) by mixing 5% (v/v) DMSO (5 wt%) in the poly(ethlylenemine)-PEDOT:PSS. A further concentration increase in DMSO (10 v/v %) decreased the conductivity of the yarn (1.5 S cm<sup>-1</sup>). Although the conductivity of our yarn (70% cotton and 30% polyethylene) was much lower than other candidates, such as poly(ethylene terephthalate) (PET) and polyester, we selected this cotton-rich yarn because of its extremely large surface for bacteria to attach, which considerably reduces the internal resistance of the MFC and improves the output power. Because MFC power output does not decline significantly while internal resistance is about  $k\Omega$ , yarn with only tens of Ohms should not be affected. The inserted Ag<sub>2</sub>O in the PEDOT:PSS works as a cathodic catalyst, which reduces Ag<sub>2</sub>O to Ag by collecting the protons and the electrons that traveled from the anode in the following reaction,

$$Ag_2O + 2H^+ + 2e^- \rightarrow 2Ag + H_2O$$
 (1)

The microbial fuel cell horizontally structured in the 1-D yarn can be the most favorable platform for wearable applications because of its lightweight and easy integrability into other wearable textiles. Above all, mechanical flexibility is one of the outstanding properties of the device. The 1-D yarn device sustained various mechanical deformations, including bending, knotting, looping, and winding without rupture (Fig. 1C). To operate the device, bacterial inoculum in a liquid is dropped on the anodic region of the yarn, flowing through the entire





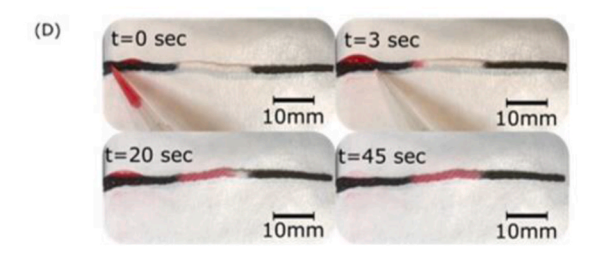


**Fig. 1.** The basic properties of 1-D microbial fuel cell. (A) The components of 1-D device consisting of anode (*A*) and cathode (*C*), separated by ion exchange channel (*I*). The anode was made with PEDOT:PSS, DMSO, and PEI while the cathode was coated with the mixture of PEDOT:PSS and silver (I) oxide. (B) The electrical conductivity of the anode with different concentration of materials. (C) The 1-D device under various mechanical deformations, including bending, knotting, looping, and winding without rupture. (D) The wicking property of the 1-D device.

yarn device (Fig. 1D). While bacterial cells remained in the anode because of the flow obstruction from the fibrous yarn network structure, the ionic media smoothly flow to the pristine region and the cathode through the capillary action (Fig. 2A). As shown in scanning electron microscope (SEM) images, bacterial cells were not found in the middle channel and cathode. This liquid transport along the yarn enables the anode, ionic exchange channel, and cathode to perform efficiently. The capillary flow in the yarn follows Washburn's equation,

$$L = \sqrt{\frac{(\gamma cos\theta)Dt}{4\mu}} \tag{2}$$

where L is the length of wetted yarn,  $\gamma$  and  $\theta$  are the interfacial tension and the contact angle between the liquid and the surface of the yarn, respectively,  $\mu$  is the viscosity of the fluid, D is the effective length of wicking, and t is the migration time of fluid [23]. Without device components including anode and cathode, the pristine yarn showed very

slow flow speed (triangle with blue dot line) while the same yarn with hydrophilization using a plasma treatment significantly improved the flow speed (rectangle with green dot line) (Fig. S1). Our yarn-based microbial fuel cell with anodic and cathodic PEDOT:PSS treatment showed the flow speed between these two yarns. A red food dye solution dropped on the anode showed the flow speed along the yarn when the ends were treated with PEDOT:PSS. The wetting traveled about 17 mm after 45 s (Fig. 1D and Movie S1). As shown in Fig. S1, we recorded the wetting distance L as a function of t (filled red circles with error bars) and compared it to the theoretical model (red line). Our experimental data showed a close correlation with the model.

Supplementary video related to this article can be found at https://doi.org/10.1016/j.jpowsour.2020.229271

 $80~\mu L$  of Shewanella oneidensis MR-1 culture with an optical density at  $600~nm~(OD_{600})$  of 2.8, corresponding to a bacterial density of about 1.4  $\times~10^9$  cells/mL, was dropped on the 25 mm-anode. Many bacterial cells remained attached to the polymer-treated yarn fibers on the anode while

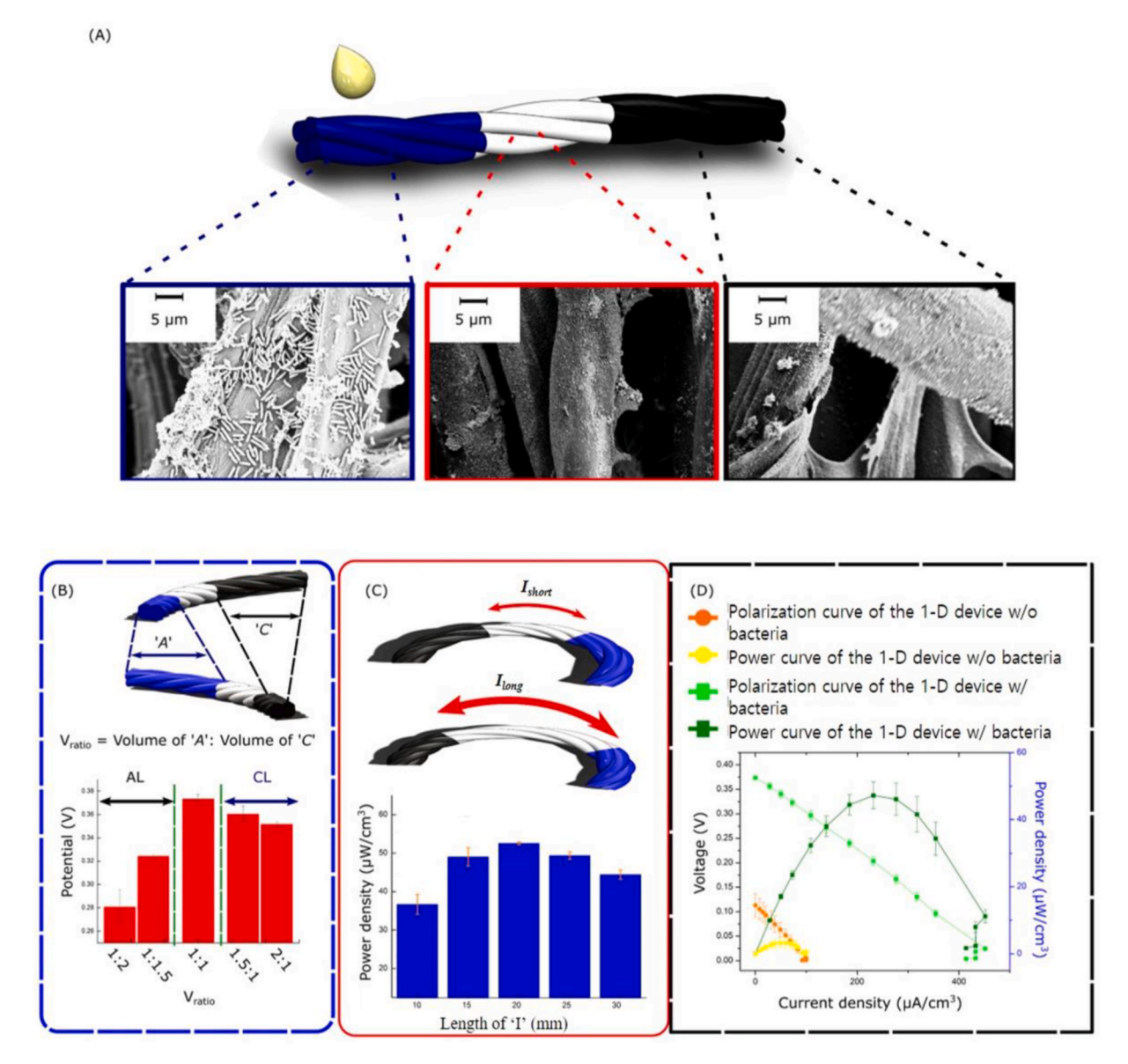


**Fig. 2.** 1-D yarn-based microbial fuel cell. (A) SEM images of each component in the single 1-D device. (B) The open circuit voltages of the microbial fuel cells with different anode to cathode length ratios. (C) Maximum power density of the devices with different lengths of 'T'. (D) Polarization curves and power outputs of the 1-D device with and without bacteria

the other ionic media flowed along the yarn, wicking through the 20 mm ionic exchange channel and the 25 mm cathode (Fig. 2A). The PEDOT: PSS treatment offered a great bacterial density at the anode and electrocatalytic activities at both electrodes because of its polymeric redox properties. Optimizing the anode and cathode length ratio can be important to maximize the device performance. We prepared five microbial fuel cells making the anode and cathode length ratios to be 1/ 1.5, 1/2, 1/1, 1.5/1, and 2/1, respectively, while the length of the ion exchange channel remained constant as 20 mm (Fig. 2B). The 1:1 ratio has a 25 mm anode and a 25 mm cathode. The microbial fuel cells with the anode to cathode length ratio below 1 (i.e. 1/1.5 and 1/2) were termed as anode-limiting devices while the MFCs with ratios above 1 (i. e. 1.5/1 and 2/1) were termed as cathode-limiting ones. Given that the open-circuit voltage (OCV) determines the overall device output voltage and power, the device performance with the different ratios can be evaluated by measuring the OCV values. 1:1 ratio generated the largest OCV while anode-limiting and cathode-limiting devices showed smaller output values. In this 1-D yarn-based configuration, the anode length was a more limiting factor than the cathode length, demonstrating that

bacterial electrochemical activity limits device performance while the solid-state Ag<sub>2</sub>O cathode provides efficient cathodic reactions. The length of the ion exchange channel is another important parameter that can affect device performance (Fig. 2C). The ion exchange channel transports protons and functions as a separator between anode and cathode. Therefore, a short length of the channel is required to reduce proton traveling distance and the overall internal resistance while a long length is required for effective separation of reactants in anode and cathode. We measured the power generation of the microbial fuel cell with different lengths of the channel from 10 mm to 30 mm while anode and cathode lengths were consistently maintained (Fig. 2C). Because their performance evaluation requires measurement of the ion transport in the different length of the channel, the OCV monitoring cannot be the right assessing tool. The shortest 10 mm channel generated smaller power than the 20 mm channel even though the short length should have reduced internal resistance. This is mainly because the short length channel could not effectively act as a separator allowing leakage of the anolyte to the cathode and lowering the overall power output. The 30 mm channel was too long to transport ions from the anode to the

cathode, reducing the performance. The maximum performance was obtained when the channel length was 20 mm. Microbial fuel cell performance was characterized by the voltage drop across the external resistor as a function of the current. By sweeping out a range of external resistors from 470, 249, 163, 100, 71.4, 47.5, 32.2, 22.1, 15.1, 10.0, 2.00, 1.55, 0.45, to  $0.36 \text{ k}\Omega$ , a current vs. voltage curve (referred to as a polarization curve) was obtained, from which a power output curve was calculated as a function of current (Fig. 2D). Normally, the polarization curve is used to characterize the OCV of the device and its internal resistance components (i.e. activation, ohmic, and mass transfer losses) while the power output curve shows the maximum power value of the device at which the external resistance becomes identical to the internal resistance of the device [24]. With the optimized length of the channel (20 mm) and the ratio of the anode to the cathode (1:1), the 1-D single varn microbial fuel cell produced the maximum current and power density of 452  $\mu$ A/cm<sup>3</sup> (at 2 k $\Omega$ ) and 47.2  $\mu$ W/cm<sup>3</sup> (at 32.3 k $\Omega$ , corresponding to the internal resistance of the device), which is much higher than the recent two-yarn microbial fuel cell (Fig. 2D) [17]. Our single varn device could more effectively transport ions smoothly from the anode to the cathode while the previous two-varn device had two functional varns wound on the core cord, leading to three physical barriers for the ions between the anode, the cord and the cathode. Even with the mechanical bending (180° to 90°), the 1-D yarn device demonstrated a stable performance within the range of only 7.25% variation in current outputs (Fig. S2).

## 2.2. Serial and parallel connection of 1-D microbial fuel cells

Increasing the voltage output without using a DC/DC booster or a charge pump requires the series connection of the microbial fuel cells to

supply an operating voltage enough for electronic applications. Many of our horizontally structured microbial fuel cells can be readily integrated into a single yarn forming an in-series connection (Fig. 3A-I and Fig. S3). Multiple device sets consisting of anodes, cathodes and pristine regions were repeatedly prepared along a single yarn where each device was spatially-distinct. A cathode of one device and an anode of the next device were electrically connected by coating the varn with the graphite ink between the two neighboring devices while the bacterial sample dropped on one device was not shared with the other devices because of the hydrophobicity of the ink. Therefore, the liquid sample was contained within the device, not transported to the other neighboring devices, leading to an in-series connection between independently working microbial fuel cells. We demonstrated a series connection of two and three microbial fuel cells formed on a single yarn and compared their performance to a single microbial fuel cell. From the polarization and power curves shown in Fig. 3A-II, the performances of a single device and its stacks in series were characterized. The OCVs increased to 619 mV for the double microbial fuel cell stack, and 989 mV for the triple device stack, compared to 373 mV obtained from a single microbial fuel cell. The maximum power of 3.72 µW in the triple-device stack surpassed 1.29 µW for the single device by a factor of 2.9. These results indicate that a series connection of multiple microbial fuel cells on a single 1-D yarn was successfully established. To further evaluate the efficiency of the device, a cyclic voltammetric analysis was conducted by using a two-electrode mode without a reference electrode (Fig. S4). The working electrode (W) was connected to the anode and the reference (R) and the counter (C) electrodes were connected to the cathode. Because no reference electrode is available in real devices and the two-electrode mode measures the complete current flow with a voltage sweep across the whole electrochemical cell, this two-electrode experiment can

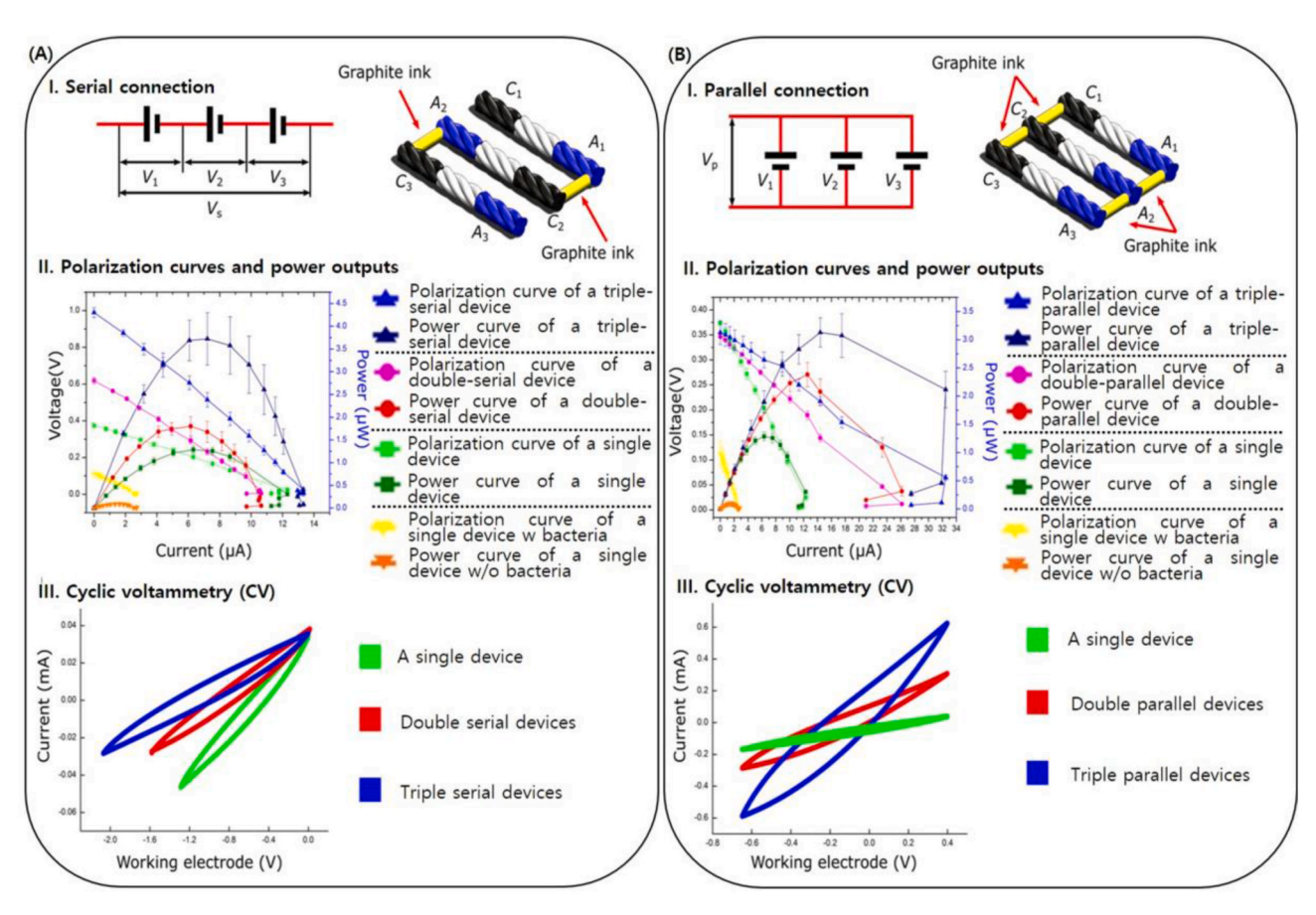


Fig. 3. Serial and parallel connection of 1-D microbial fuel cells. (A) Serial connection. I. Schematic illustrations of the serial connection of the 1-D device, II. Polarization curves and power outputs, and III. CV curves. (B) Parallel connection. I. Schematic illustrations of parallel connection of the 1-D device, II. Polarization curves and power outputs, and III. CV curves.

reflect the actual efficiency of the cell. Under the different scanned window potentials in terms of the number of cells connected in series, the current between the anode and cathode was measured. The sweep potential was 50 mV/s. Smaller currents were observed from the two-and three-device stacks on each window of the scanned potential than the single microbial cell without serial connection (Fig. 3A–III). This is mainly because of the imbalanced distribution of the individual devices' performances. The device with the least performance can induce a reversal of the cell voltage to the negative and limit the current flow of the entire stack [25,26]. This issue can be critical in practical applications because the serial connection can reduce the overall power performance. Therefore, the serial stacking of the microbial fuel cells needs to be carefully assembled without the internal resistant mismatch, imbalance of substrate loading, and variation in manufacturing.

The parallel connection of the microbial fuel cells can also be readily established by clipping together all anode and cathode termnals, respectively (Fig. 3B–I and Fig. S3). The connection of two and three device units in parallel produced the maximum current of 23.3  $\mu A$ , and 32.5  $\mu A$ , respectively, while the single device generated only 12.3  $\mu A$  (Fig. 3B–II). The maximum power of 2.38  $\mu W$  and 3.13  $\mu W$  in the two-and three-parallel stack, respectively, surpassed 1.28  $\mu W$  for the single device. The parallel stacks of the devices produced the same OCV as the single one without connection. The cyclic voltammetry measurements demonstrate the increasing magnitude of current with the number of

connections (Fig. 3B–III). Although the performance of the individual units in the stack was not measured, it should be noted that energy loss can be substantial because of unequal OCVs in parallelly stacked units, similar to the energy loss in a serially stacked device [27]. The energy and power reduction can occur until the voltage output in a high OCV unit is equal to the other units having low OCV. Therefore, the parallel stack of the devices also needs to be assembled carefully to minimize energy loss. Our system does not provide any malfunction due to the individual unit's performance mismatch and subsequent voltage reversals [28].

## 2.3. 2-D and 3-D microbial fuel cells

The concept of the horizontally structured microbial fuel cell can be readily extended to 2-D and 3-D woven fabric formats (Fig. 4). Interlacing functional components in the form of 1-D yarn into 2-D and 3-D fabrics or textiles can be the simplest and the most convenient technique to enable the complete function of the smart textile. Anodic and cathodic yarns were first prepared by coating the entire yarns with individual functional materials, and then interfaced as weft yarns into the 2-D woven anode and cathode with pristine yarns as warp yarns (Fig. 4A). The large anode and cathode regions (28.5 mm  $\times$  28.5 mm, each) were separated by 20 mm from the pristine yarns, which ultimately formed the horizontally structured microbial fuel cell in 2-D. The

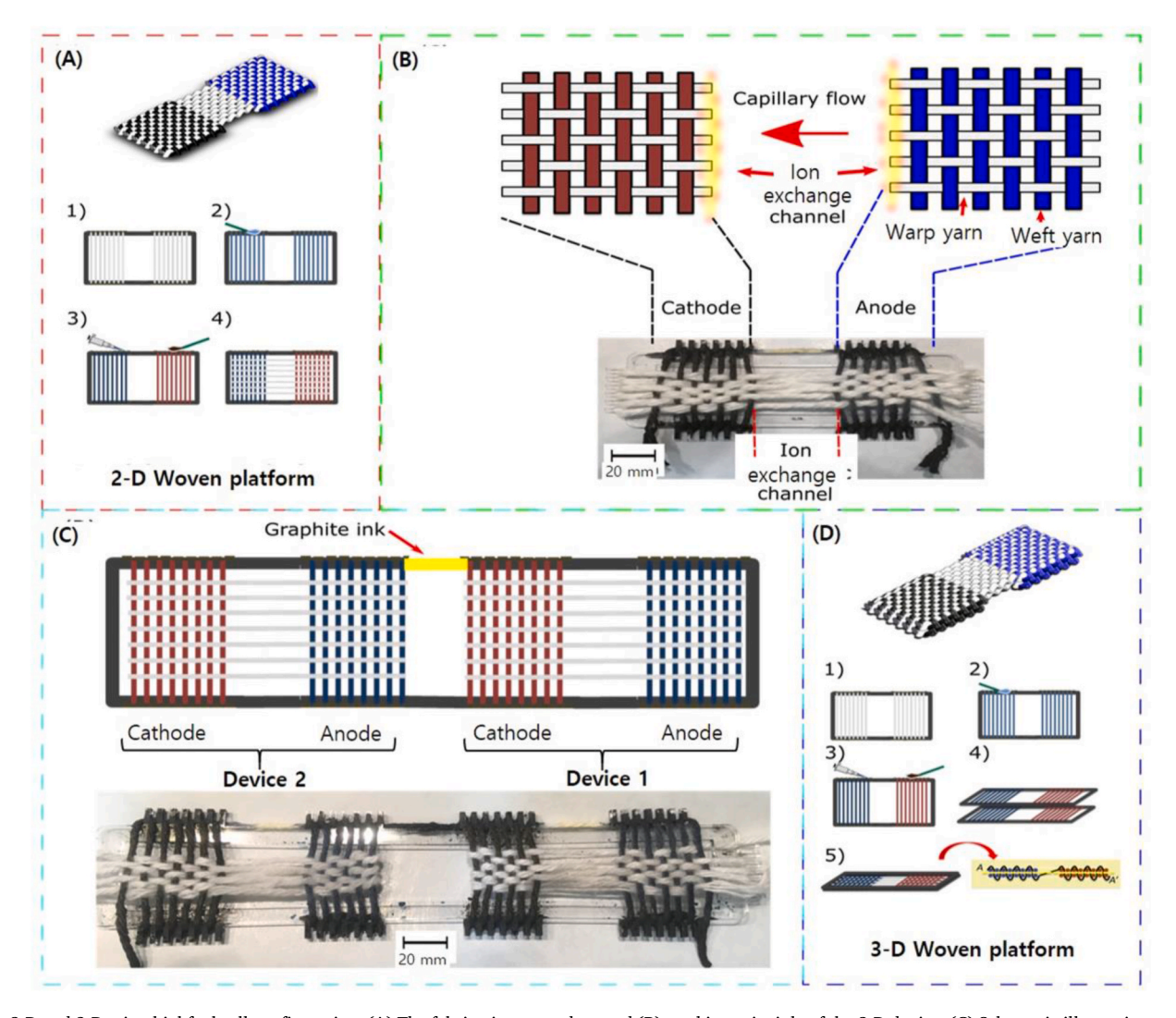


Fig. 4. 2-D and 3-D microbial fuel cell configuration. (A) The fabrication procedure and (B) working principle of the 2-D device. (C) Schematic illustration and photo image of the two microbial fuel cells connected in series. (D) The fabrication process of the 3-D microbial fuel cell.

pristine yarns functioned as the ion exchange channels to transport protons from the anode to the cathode and simultaneously acted as the physical and chemical separator between the electrodes (Fig. 4B). The serial connection of the 2-D microbial fuel cell was fulfilled by repeatedly interlacing those functional yarns along the warp pristine yarns and electrically connecting the cathode of one unit and the anode of the next unit (Fig. 4C). The parallel connection was realized by weaving 2-D layer devices in the vertical direction, forming a 3-D microbial fuel cell stack (Fig. 4D). A through-the-thickness binder yarn along the Z axis was interlaced with the warp and weft yarns in in-plane directions to provide 3-D structural integrity.

About 1 mL of bacterial culture was dropped on each anodic region of the 2-D woven fabric. The CV was first measured to evaluate the current generation by scanning the potential from -1.35 V to 0 V at a scan rate of 5 mV/s (Fig. 5A). Much greater current was observed from this 2-D microbial fuel cell than the 1-D device. Moreover, the OCV of the 2-D device was about 493 mV and its maximum power and current was 5.66 µW and 34.0 µA, respectively, which is significantly greater than the 1-D yarn-based microbial fuel cell having 373 mV (OCV), 1.29 μW (maximum power) and 12.3 μA (maximum current), respectively (Fig. 5B). When the two 2-D devices were serially connected, the OCV increased to 984 mV while the maximum power and current were raised to 11.8 µW and 43.0 µA, respectively. Connecting the two seriallyconnected 2-D devices in parallel formed the 3-D microbial fuel cell stack and increased total current and power generation to 17.4  $\mu W$  and  $65.6 \mu A$ , respectively. The OCV (984 mV) of the 3-D structured device with the parallel connection of the two serial devices was similar to the

two serial 2-D devices. About 2 mL of bacterial sample was introduced to the anode of the 3-D device. The 2-D and 3-D woven structured microbial fuel cells exhibited much greater and more stable operation in generating electricity. To further increase the power output, we stacked two three-series-connected microbial fuel cells in parallel into the 3-D woven fabric (Fig. 5C). This stack delivered a maximum power of 70.3  $\mu W$ , which is more than enough electrical energy to power an electrical calculator (Fig. 5C, Fig. S5, and Movie S2). This is the first demonstration of the textile microbial fuel cell as a real-world wearable power source.

Supplementary data related to this article can be found at https://doi.org/10.1016/j.jpowsour.2020.229271.

## 2.4. Future works

In our previous report, we ensured the practical efficacy of the skininhabiting bacteria as a novel and sole sweat-based energy harvesting device for wearable applications [14]. Those bacteria will can incorporated into the yarn- and fabric-based microbial fuel cells we developed here in this work. Although the proposed conceptual technique is at the beginning stage and the issue of microbial cytotoxicity must be addressed for the actual applications, it can be an entirely new area of energy harvesting research and revolutionize the way of powering wearable applications. The horizontally structured microbial fuel cells in 1-D yarn and 2-D/3-D woven fabrics will function as a power supply by tightly attaching to the human skin and effectively absorbing the sweat as a bacterial energy source in the anode and an ionic electrolyte

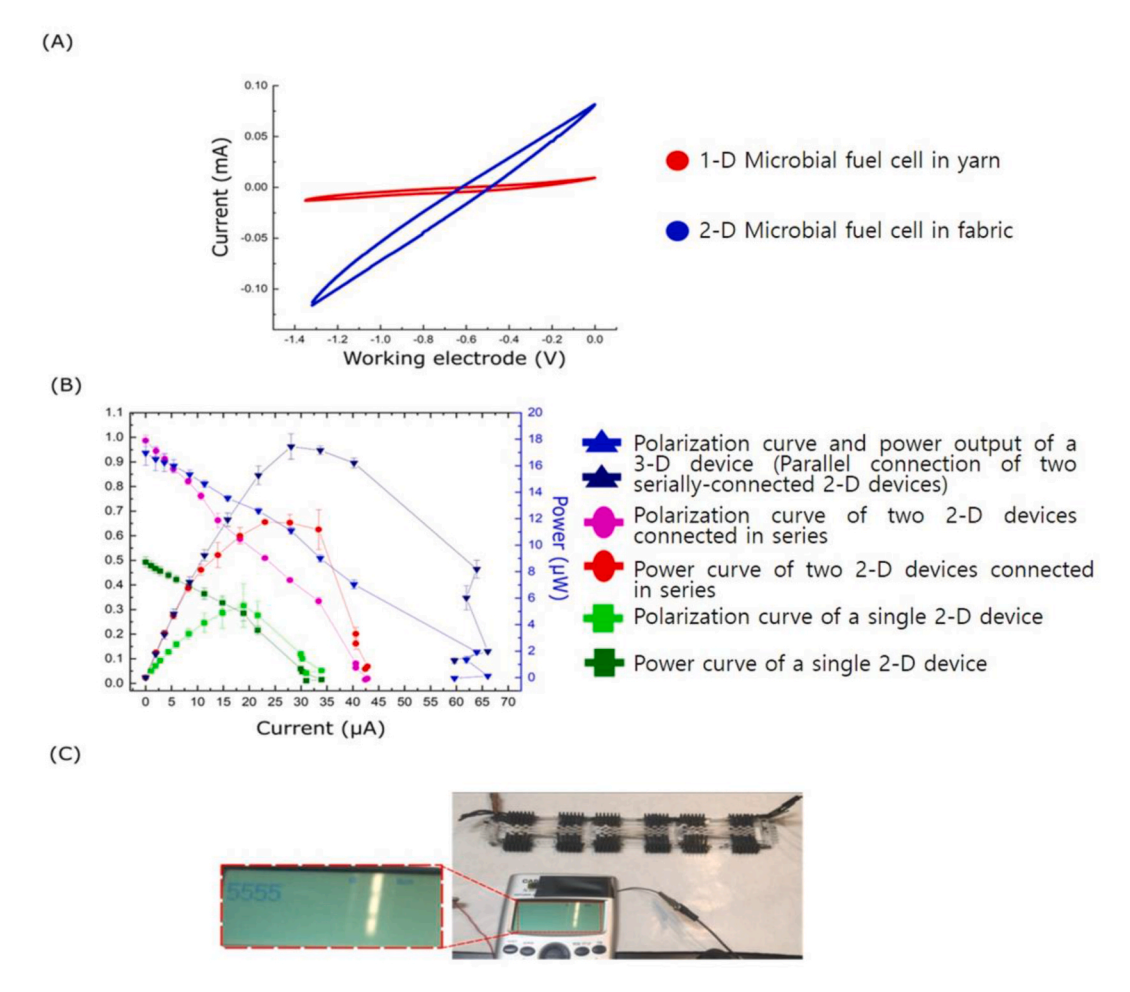


Fig. 5. Performance of 2-D and 3-D microbial fuel cells. (A) CV curves of the 1-D and 2-D devices. (B) Polarization curves and power outputs of the serially and parallely connected fabric devices. (C) Photos of the 3-D device pack with pallel connection of three serially-connected 2-D devices, powering the electrical calculator.

in the ion exchange channel. Electrogenic skin bacteria will be gathered from the host and be inoculated in the device. In that way, we expect a minimal foreign-body response. Or other electrogenic bacteria obtained from outside the host can be carefully integrated and immobilized in the anode, generating power with human sweat. In this case, a tight and innovative packaging technology will be required to prevent those bacteria from leaking to the host and posing a health concern. Although the current work mainly focused on the new device architecture on the flexible and stretchable yarns and fabrics for potential wearable applications, it will push forward the frontiers of wearable electrochemical bioenergy harvesting and will soon revolutionize wearable technology.

#### 3. Conclusion

In this work, we created a novel architecture of the microbial fuel cell horizontally structured in 1-D yarn and 2-D/3-D woven fabrics, which can provide new opportunities for the development of wearable bioenergy harvesters in the next generation of smart textiles. This horizontal configuration can be readily fabricated in the yarns and fabrics by coating functional materials and using simple series and parallel connections along the 1-D yarn or horizontally throughout the 2-D fabric and vertically through the 3-D structure. Furthermore, the excellent wicking force of the hydrophilic yarns and fabrics could contain and transport aqueous reagents such as bacterial inoculum and electrolyte, allowing efficient device operation potentially on human skin by absorbing sweat. The well-known exoelectrogen, Shewanella oneidensis MR-1, used as biocatalysts in the yarn- and fabric-based microbial fuel cells, produced great power and current. The three-dimensionally structured device that stacked two three-series-connected packs in parallel successfully powered an electrical calculator. In its current phase, this work represents a major step toward a versatile scalable design of wearable energy-generating devices and shows the potential for practical, portable applications.

# 4. Experimental section

## 4.1. Preparation of functional electrodes

A commercially available yarn composed of 70% cotton and 30% polyethylene terephthalate was immersed in 70 v/v% ethanol and sonicated for 30 min, followed by drying in a ventilated oven at 80 °C to sterilize the yarns and to remove grease that could make it water repellent. To functionalize a 1-D yarn with anodic and cathodic materials, we fixed the cleaned varns in the grooves to hold them firmly in tension on a polymethylmethacrylate (PMMA) frame engraved by a laser cutter (VLS 3.5 from Universal laser systems). We coated each end of the varn with anodic and cathodic materials, respectively. The anodic ink was prepared by mixing poly(3,4-ethylenedioxythiophene):polystyrene sulfonate (PEDOT:PSS, Clevios PH1000 from Heraeus) with dimethyl sulfoxide (DMSO from Sigma-Aldrich). The addition of the DMSO, which is a polar solvent separated the phase between PEDOT and PSS, resulting in greater conductivity upon drying. The introduction of the poly(ethlylenemine) (PEI from Sigma-Aldrich) to the anodic ink improved the electrochemical reactions. For the cathodic material, a silver-based paste was prepared by mixing silver (I) oxide (Sigma-Aldrich) with 1 wt% PEDOT:PSS by the ratio of 45 mg/mL and sonicating them for 60 min. For the planar 2-D microbial fuel cell, functional anodic and cathodic yarns were first prepared in a similar way as the 1-D device. Single non-treated yarns were fixed in the PMMA grooves and were coated with anodic and cathodic materials, respectively, along the entire yarns. Non-treated pristine yarns were then fixed as warp yarns on the new PMMA grooves and those functional yarns were woven as weft yarns into a large conductive fabric anode and cathode. The pristine fabric region was designed to be placed between them, forming a horizontally structured 2-D microbial fuel cell. The 2-D devices were connected in series by linking the anode of one device and the cathode of the next one with graphite ink. For a 3-D microbial fuel cell with parallel connections between the 2-D devices, a through-the-thickness conductive binder yarn was interlaced in the vertical direction.

## 4.2. Inoculum preparation

Shewanella oneidensis MR-1 was grown from  $-80~^{\circ}\text{C}$  glycerol stock cultures by inoculating 20 mL of Luria broth (LB) medium consisting of 10 g of tryptone, 5.0 g of yeast extract, and 5.0 g of NaCl per liter of DI water. The *S. oneidensis* MR-1 in media was cultured for 24 h until the OD<sub>600</sub> reached 2.8 for inoculation as anolyte.

## 4.3. Data acquisition and measurement setup

The potential difference between the anode and cathode was measured by a data acquisition system to record the voltage output every 1 min when the S. oneidensis MR-1 inoculum was dropped to the anode. While the bacterial cells remained in the anode, other ionic liquid flowed to the cathode along the pristine yarn, which formed an ionic exchange pathway. A custom-built interface system (DI-4108U from DATAQ Instruments) was linked to a personal computer to measure the electrical outputs driven by the bacterial metabolism as a function of time. The OCV of the device was first measured to establish the base device performance. To determine the current generated by the device, external resistors were used to connect the anode and cathode, where the current flow through the resistor was calculated by Ohm's law. The current and power density of the 1-D microbial fuel cell were calculated and normalized by the volume of the anode. For the further electrochemical evaluation of the devices, we conducted the cyclic voltammetry (CV) measurement (Squidstat Plus from Admiral Instruments) by using a two-electrode mode composed of the working electrode and a combination reference and counter electrode (Fig. S4). In the electrochemical system, the testing object was a working electrode, while the counter electrode was set to complete the electrical circuit. Three CV scans were performed ensuing the electrode sample fabrication and the third CV scan from difference samples was used for comparison. The resistivities of the 1-D yarn were measured by the custom-built tool that had a four-point setup (Fig. S6). The conductivity  $(\sigma)$  was calculated from the measured voltage (V) from the inner two probes and the applied current (I) through the outer two probes according the equation below:

$$\sigma = \frac{IL}{V\pi r^2} \tag{4}$$

where the distance (L) between the two inner probes was 1 cm, r was the fiber radius [17,29].

# 4.4. Bacterial fixation and SEM imaging

To take SEM images, inoculated cells in the yarn were fixed with 4% glutaraldehyde solution in 0.1 M phosphate buffer saline (PBS) overnight at 4  $^{\circ}\text{C}$ . The fixing reagent was rinsed three times with 0.1 M PBS. To dehydrate the cells, the yarn was put through the series of baths made up of 35%, 50%, 75%, 95%, and 100% ethanol. Finally, it was immersed in hexamethyldisilazane (HMDS), a highly volatile organic compound, for 10 min to minimize the distortion. Immediately afterward, the samples were placed in a desiccator and dried overnight. Fixed cells were examined using a field emission SEM (Supra 55 VP from Zeiss).

# CRediT authorship contribution statement

**Jihyun Ryu:** Investigation, Methodology, Data curation, Writing - original draft. **Yang Gao:** Investigation, Formal analysis. **Jong Hyun Cho:** Investigation, Formal analysis. **Seokheun Choi:** Conceptualization, Supervision, Project administration, Funding acquisition, Writing -

original draft, Writing - review & editing, finalization.

## Declaration of competing interest

The authors declare that they have no known competing financial interests or personal relationships that could have appeared to influence the work reported in this paper.

## Acknowledgments

This work was supported by the National Science Foundation (ECCS #1920979 & #2020486), Office of Naval Research (#N00014-81-1-2422), Integrated Electronics Engineering Center (IEEC), and the SUNY Binghamton Research Foundation (SE-TAE). The authors would like to thank the Analytical and Diagnostics Laboratory (ADL) at SUNY-Binghamton for providing the fabrication facilities.

# Appendix A. Supplementary data

Supplementary data related to this article can be found at https://doi.org/10.1016/j.jpowsour.2020.229271.

### References

- Y. Pang, Z. Yang, Y. Yang, T.L. Ren, Wearable electronics based on 2D materials for human physiological information detection, Small 16 (2020) 1901124.
- [2] H.R. Lim, H.S. Kim, R. Qazi, Y.T. Kwon, J.W. Jeong, W.H. Yeo, Advanced soft materials, sensor integrations, and applications of wearable flexible hybrid electronics in healthcare, Energy Environ. Adv. Mater. 32 (2020) 1901924.
- [3] X. Wang, L. Dong, H. Zhang, R. Yu, C. Pan, Z.L. Wang, Recent progress in electronic skin, Adv. Sci. 2 (2015) 1500169.
- [4] S. Wang, J.Y. Oh, J. Xu, H. Tran, Z. Bao, Skin-inspired electronics: an emerging paradigm, Acc. Chem. Res. 51 (2018) 1033–1045.
- [5] K. Hu, R. Xiong, H. Guo, R. Ma, S. Zhang, Z.L. Wang, V.V. Tsukruk, Self-powered electronic skin with biotactile selectivity, Adv. Mater. 28 (2016) 3549–3556.
  [6] H. He, H. Zeng, Y. Fu, W. Han, Y. Dai, L. Xing, Y. Zhang, X. Xue, A self-powered
- [6] H. He, H. Zeng, Y. Fu, W. Han, Y. Dai, L. Xing, Y. Zhang, X. Xue, A self-powered electronic-skin for real-time perspiration analysis and application in motion state monitoring, J. Mater. Chem. C 6 (2018) 9624–9630.
- [7] G. Chen, Y. Li, M. Bick, J. Chen, Smart textiles for electricity generation, Chem. Rev. 120 (2020) 3668–3720.
- [8] Y. Yu, J. Nassar, C. Xu, J. Min, Y. Yang, A. Dai, R. Doshi, A. Huang, Y. Song, R. Gehlhar, A.D. Ames, W. Gao, Biofuel-powered soft electronic skin with multiplexed and wireless sensing for human-machine interfaces, Sci. Robotics 5 (2020), eaaz7946.
- [9] A.J. Bandodkar, J. You, N. Kim, Y. Gu, R. Kumar, A.M. Vinu Mohan, J. Kurniawan, S. Imani, T. Nakagawa, B. Parish, M. Parthasarathy, P.P. Mercier, S. Xu, J. Wang, Soft, stretchable, high power density electronic skin-based biofuel cells for scavenging energy from human sweat, Energy Environ. Sci. 10 (2017) 1581–1589.

- [10] J. Lv, I. Jeerapan, F. Tehrani, L. Yin, C.A. Silva-Lopez, J. Jang, D. Joshuia, R. Shah, Y. Liang, L. Xie, F. Soto, C. Chen, E. Karshalev, C. Kong, Z. Yang, J. Wang, Sweat-based wearable energy harvesting-storage hybrid textile devices, Energy Environ. Sci. 11 (2018) 3431–3442.
- [11] J. Choi, R. Ghaffari, L.B. Baker, J.A. Rogers, Skin-interfaced systems for sweat collection and analysis, Sci. Adv. 4 (eaar3921) (2018).
- [12] M.H. Osman, A.A. Shah, F.C. Walsh, Recent progress and continuing challenges in bio-fuel cells. Part I: enzymatic cells, Biosens. Bioelectron. 26 (2011) 3087–3102.
- [13] M.H. Osman, A.A. Shah, F.C. Walsh, Recent progress and continuing challenges in bio-fuel cells. Part II: microbial cells, Biosens. Bioelectron. 26 (2010) 953–963.
- [14] M. Mohammadifar, M. Tahernia, J.H. Yang, A. Koh, S. Choi, Biopower-on-Skin: electricity generation from sweat-eating bacteria for self-powered e-skins, Nano Energy 75 (2020) 104994.
- [15] S. Pang, Y. Gao, S. Choi, Flexible and stretchable biobatteries: monolithic integration of membrane-free microbial fuel cells in a single textile layer, Adv. Energy Mater. 8 (2018) 1702261.
- [16] S. Pang, Y. Gao, S. Choi, Flexible and stretchable microbial fuel cells with modified conductive and hydrophilic textile, Biosens. Bioelectron. 100 (2018) 504–511.
- [17] Y. Gao, J.H. Cho, J. Ryu, S. Choi, A scalable yarn-based biobattery for biochemical energy harvesting in smart textiles, Nano Energy 74 (2020) 104897.
- [18] Y. Gao, S. Choi, Merging electric bacteria with paper, Adv. Mater. Technol. 3 (2018) 1800118.
- [19] M.M. Hamedi, A. Ainla, F. Guder, D.C. Christodouleas, M. Fernandez-Abedul, G. M. Whitesides, Integrating electronics and microfluidics on paper, Adv. Mater. 28 (2016) 5054–5063.
- [20] G.B. Tseghai, D.A. Mengistie, B. Malengier, K.A. Fante, L. Van Langenhove, PEDOT: PSS-based conductive textiles and their application, Sensors 20 (2020) 1881.
- [21] W. Cai, T. Österberg, M.J. Jafari, C. Musumeci, C. Wang, G. Zuo, X. Yin, X. Luo, J. Johansson, M. Kemerink, L. Ouyang, T. Ederth, O. Inganäsb, Dedoping-induced interfacial instability of poly(ethylene imine)s-treated PEDOT:PSS as a low-work-function electrode, J. Mater. Chem. C 8 (2020) 328–336.
- [22] L.V. Lingstedt, M. Ghittorelli, H. Lu, D.A. Koutsouras, T. Marszalek, F. Torricelli, N. I. Crăciun, P. Gkoupidenis, P.W.M. Blom, Effect of DMSO solvent treatments on the performance of PEDOT:PSS based organic electrochemical transistors, Adv. Electron. Mater. 5 (2019) 1800804.
- [23] R. Safavieh, G.Z. Zhou, D. Juncker, Microfluidics made of yarns and knots: from fundamental properties to simple networks and operations, Lab Chip 11 (2011) 2618.
- [24] A. Fraiwan, S.P. Adusumilli, D. Han, A.J. Steckl, D.F. Call, C.R. Westgate, S. Choi, Microbial power-generation capabilities on micro-/nano-structured anodes in micro-sized microbial fuel cells, Fuel Cell. 14 (2014) 801–809.
- [25] S. Choi, J. Chae, An array of microliter-sized microbial fuel cells generating 100 μW of power, Sensor Actuator Phys. 177 (2012) 10–15.
- [26] S.E. Oh, B.E. Logan, Voltage reversal during microbial fuel cell stack operation, J. Power Sources 167 (2007) 11–17.
- [27] J.B. Benziger, M.B. Satterfield, W.H.J. Hogarth, J.P. Nehlsen, I.G. Kevrekidis, The power performance curve for engineering analysis of fuel cells, J. Power Sources 155 (2006) 272–285.
- [28] B. Kim, S.V. Mohan, D. Fapyane, I.S. Chang, Controlling voltage reversal in microbial fuel cells, Trends Biotechnol. 38 (2020) 667–678.
- [29] T. Hou, J.P. Lynch, Electrical impedance tomographic methods for sensing strain fields and crack damage in cementitious structures, J. Intell. Mater. Syst. Struct. 20 (2009) 1363–1379.